METHODS AND APPLICATIONS OF ANALYSIS.
Vol. 16, No. 3, pp. 341–364, September 2009

005

A PARADIGM FOR TIME-PERIODIC SOUND WAVE PROPAGATION IN THE COMPRESSIBLE EULER EQUATIONS*

BLAKE TEMPLE† AND ROBIN YOUNG‡

Abstract. We formally derive the simplest possible periodic wave structure consistent with time-periodic sound wave propagation in the 3×3 nonlinear compressible Euler equations. The construction is based on identifying the simplest periodic pattern with the property that compression is counter-balanced by rarefaction along every characteristic. Our derivation leads to an explicit description of shock-free waves that propagate through an oscillating entropy field without breaking or dissipating, indicating a new mechanism for dissipation free transmission of sound waves in a nonlinear problem. The waves propagate at a new speed, (different from a shock or sound speed), and sound waves move through periods at speeds that can be commensurate or incommensurate with the period. The period determines the speed of the wave crests, (a sort of observable group velocity), but the sound waves move at a faster speed, the usual speed of sound, and this is like a phase velocity. It has been unknown since the time of Euler whether or not time-periodic solutions of the compressible Euler equations, which propagate like sound waves, are physically possible, due mainly to the ubiquitous formation of shock waves. A complete mathematical proof that waves with the structure derived here actually solve the Euler equations exactly, would resolve this long standing open problem.

Key words. Periodic solution, shock free, shock, nonlinear waves, group velocity, signaling, Euler equations, compressible flow.

AMS subject classifications. 35L65, 35L67, 70K30, 74H05, 74J30

1. Introduction.

Since Euler derived the equations in 1752, it has been an open problem whether or not time periodic solutions of the compressible Euler equations exist, and what the nature of their structure is if they do exist. Euler's derivation established the theory of music and sound when he linearized the equations and obtained the same wave equation in the pressure that his colleague D'Alembert had obtained several years earlier to describe the vibrations of a string. Yet to this day it is still unknown whether or not the fully nonlinear equations support time-periodic solutions analogous to the sinusoidal oscillations of the linear theory [3]. After Riemann demonstrated in 1858 that shock waves can form in smooth solutions of the equations, most experts have believed that time periodic solutions of the compressible Euler equations, (that propagate like sound waves), were not mathematically possible due to the formation of shock waves, [24][1]. The basic intuition is that, when a periodic wave is nonlinear, each period will decompose into a *rarefactive* region, (characteristics spreading out in forward time), and a *compressive* region, (characteristics impinging in forward time), and in the compressive part the "back will catch up to the front", causing it to break, (something like a wave breaking on the beach), forming a shock-wave; then the wave amplitude will decay to zero by shock-wave

*Received June 10, 2009; accepted for publication October 7, 2009.

†Department of Mathematics, University of California, Davis, CA 95616, USA (temple@math.ucdavis.edu). The first author is supported in part by NSF Applied Mathematics Grant Number DMS-040-6096.

‡Department of Mathematics and Statistics, University of Massachusetts, Amherst, MA 01003, USA (young@math.umass.edu). The second author is supported in part by NSF Applied Mathematics Grant Number DMS-050-7884.

[1]There are trivial time periodic solutions that represent entropy variations which, in the absence of dissipative effects, are passively transported. There is no nonlinear sound wave propagation in these solutions. When we speak of time periodic solutions, we always mean with nonlinear wave propagation.

dissipation. Entropy strictly increases in time like a Liapunov function when shock-waves are present, so the presence of shock-waves is inconsistent with time periodic evolution. This intuition was partially validated in the definitive work of Glimm and Lax [9], which established that when temperature or entropy is assumed constant, solutions of the resulting 2×2 system, starting from periodic initial data, must form shock waves and decay, by shock wave dissipation, at rate $1/t$.

The idea that time periodic solutions were possible for sound wave propagation through an oscillatory entropy field was kindled by work of Majda, Rosales and Schonbeck [19, 20, 21], and Pego [22], who found periodic solutions in asymptotic models of the compressible Euler equations[2]. Our work here was motivated by our own earlier work [33, 28, 27] on existence of solutions and [34, 35, 37] on model problems, and by the numerical work of Rosales, Shefter and Vaynblat [25, 31], who produced detailed numerical simulations of the Euler equations and asymptotic models starting from space-periodic initial data. These latter studies indicate that periodic solutions of the 3×3 compressible Euler equations do not decay like the 2×2 p-system, and authors make observations about the possibility of periodic, or quasi-periodic attractor solutions.

In this paper we (formally) derive the simplest wave pattern consistent with the condition that compression and rarefaction are in balance along every characteristic. To start we prove that nonlinear simple waves can change from Compressive (C) to Rarefactive (R), and back again, upon interaction with an entropy jump. We then formally classify "consistent" configurations of R's and C's with the idea of locating the simplest periodic pattern for which compression and rarefaction are in balance. From this we produce the simplest (formal) nontrivial wave configuration that balances compression and rarefaction along every characteristic. In this simplest pattern, the solution oscillates in space between two different entropy levels, and each backward and forward characteristic passes through four different compressions and four different rarefactions, crossing eight entropy levels, before it periodically returns to its initial state[3].

The authors believe that the connection between long time existence of dissipation free sound wave transmission, and the combinatorial problem of balancing compression and rarefaction along all characteristics is new, and will lead to interesting wave structures more complicated than the simplest structure derived here. Moreover, we conjecture that a solution of compressible Euler, starting from space-periodic initial data, will in general decay in time to a time periodic, or perhaps quasi-periodic solution, that balances compression and rarefaction along characteristics, and will *not* in general decay to the constant state average in each period as in [9].

In [29] we describe and solve the linearized problem associated to nonlinear periodic solutions having the structure described here and recast the fully nonlinear existence problem as a perturbation problem. We then characterize the spectrum of the linearized operator, and show that it is invertible and diagonal on the complement of its kernel, which is one-dimensional. In [30], we further reduce the problem to an Implicit Function Theorem with small divisors. We also show that periodic solutions with the wave structure derived here exist to within arbitrarily high Fourier mode

[2]See [13, 12, 16, 17] for blowup results insufficient to rule out periodic solutions, and [10, 11] for an example of a periodic solution in a quasilinear system.

[3]The discontinuities at the entropy jumps are time-reversible *contact discontinuities* which, unlike shock waves, are allowable in time-periodic solutions because they entail no dissipation, or gain of entropy, c.f. [26].

cutoff. Taken all together, we believe this constitutes what we might call a "physical" proof that periodic solutions having the wave structure we have identified exist[4].

In Section 2 we introduce the compressible Euler equations, review the Lagrangian formulation of the equations, and introduce new variables z and m useful for the subsequent analysis. In Section 3 we define Compression (C) and Rarefaction (R) along a characteristic in a general solution, and show that the R/C character does not change when the entropy is constant. In Section 4 we analyze the interaction of simple waves with a single entropy discontinuity, and show that there are exactly twelve different possible R/C patterns that characterize such interactions, and in eight of these cases one of the nonlinear waves changes its R/C character across the interaction. Our analysis shows that the R/C pattern of an interaction is uniquely determined by the signs of the t-derivatives of the Riemann invariants of the nonlinear waves on either side of the entropy discontinuity. Of the 16 possible labellings of *forward* and *backward* waves *in* and *out* of an interaction by labels of R and C, we show that precisely four of these cannot be realized in an actual solution: these are the cases in which *both* back and forward waves change their R/C character at one such interaction, which cannot happen. The result is that one family of nonlinear waves can change from compressive to rarefactive, or vice versa, upon interaction with an entropy discontinuity, only in the presence of a wave of the opposite family that transmits its R/C character through the discontinuity. Explicit inequalities on the derivatives of the Riemann invariants on either side of the entropy discontinuity are derived that determine the R/C character of all the waves in and out of the interaction. The results are recorded in Figures 4 and 5, distinguished by whether the entropy increases or decreases across the entropy jump.

In Section 5 we use the results of Section 4 to construct the simplest global periodic pattern of R/C-wave interactions consistent with the tables of R/C interactions at the entropy levels, and consistent with the condition that R's and C's are balanced along every backward and forward characteristic. We then show that this pattern is consistent with a nontrivial global periodic structure of states. We conclude with Figures 7 and 9, which provide a detailed picture, or "cartoon", of a solution consistent with this global periodic structure. Concluding comments are made in Section 6.

2. The compressible Euler equations. The compressible Euler equations describe the time evolution of the density ρ, velocity $\mathbf{u} = (u^1, u^2, u^3)$ and energy density E of a perfect fluid under the assumption of zero dissipation and heat conduction,

$$\rho_t + \operatorname{div}[\rho \mathbf{u}] = 0, \tag{1}$$

$$(\rho u^i)_t + \operatorname{div}[\rho u^i \mathbf{u}] = -\nabla p, \tag{2}$$

$$E_t + \operatorname{div}[(E+p)\mathbf{u}] = 0, . \tag{3}$$

where $E = \frac{1}{2}\rho \mathbf{u}^2 + \rho e$ is the sum of the kinetic energy $\frac{1}{2}\rho \mathbf{u}^2$, and specific internal energy e, and p is the pressure. An equation of state relating p, ρ and e is required to close the system, and we assume the equation of state for a polytropic, or gamma

[4]We draw the analogy with the regular and Mach reflection wave patterns, for which a complete mathematical proof remains an open problem.

law gas,

$$e = c_\tau T = \frac{c_\tau}{\tau^{\gamma-1}} \exp\left\{\frac{S}{c_\tau}\right\}, \tag{4}$$

$$p = -\frac{\partial e}{\partial \tau}(S,\tau). \tag{5}$$

Here $\tau = 1/\rho$ is the specific volume, S is the specific entropy determined by the second law of thermodynamics

$$de = TdS - pd\tau, \tag{6}$$

and γ denotes the adiabatic gas constant, equal to the ratio c_p/c_τ of specific heats, [4, 26]. The system of compressible Euler equations with the polytropic equation of state is fundamental to mathematics and physics, and can be derived from first principles. The gamma law relations (4) and (5) follow directly from the equipartition of energy principle and the second law of thermodynamics for a molecular gas, leading to

$$\gamma = 1 + 2/3r, \tag{7}$$

where r is the number of atoms in a molecule [15]. Equations (1)-(3) with (4), (5) are the starting point for the nonlinear theory of sound waves, and can be regarded as the essential extension of Newton's laws to a continuous medium.

For shock-free solutions, using (6), the energy equation (3) can be replaced by the *adiabatic constraint*

$$(\rho S)_t + \operatorname{div}(\rho S \mathbf{u}) = 0, \tag{8}$$

which expresses that specific entropy is constant along particle paths [26].

For sound wave propagation in one direction, the equations reduce to the 3×3 system

$$\rho_t + (\rho u)_\xi = 0, \tag{9}$$

$$(\rho u)_t + (\rho u^2 + p)_\xi = 0, \tag{10}$$

$$E_t + ((E+p)u)_\xi = 0; \tag{11}$$

and letting x denote the *material coordinate*,

$$x = \int \rho \, d\xi, \tag{12}$$

we obtain the equivalent *Lagrangian* equations

$$\tau_t - u_x = 0, \tag{13}$$

$$u_t + p_x = 0, \tag{14}$$

$$E_t + (up)_x = 0. \tag{15}$$

In the Lagrangian frame the adiabatic constraint (8) reduces to

$$S_t = 0, \tag{16}$$

which on smooth solutions can be taken in place of (15), c.f. [4, 26]. Henceforth, we base our analysis on the Lagrangian equations.

The Lagrangian system (13)-(15) has three characteristic families, and we refer to the waves in these families as 1-, 2- and 3-waves, ordered by wave speed. The 1- and 3-families are genuinely nonlinear, and we alternatively refer to waves in these families as backward (or "−") and forward (or "+") waves, respectively. The Lagrangian spatial coordinate x moves with the fluid, so in Lagrangian coordinates backward waves always propagate at negative speed, and forward waves with positive speed. The 2-wave family consists of the linear family of contact discontinuities which we refer to as entropy waves, (or 0-waves). These entropy waves are passively transported with the fluid, and so are stationary in the Lagrangian framework. In general, the nonlinear waves can compress into shock waves in forward time, but because shock waves are incompatible with periodic propagation, we restrict our attention only to smooth simple waves, c.f. [26, 12, 14].

The thermodynamic relation (6) implies

$$e_S = \frac{\partial}{\partial S} e(\tau, S) = T, \tag{17}$$

$$e_\tau = \frac{\partial}{\partial \tau} e(\tau, S) = -p, \tag{18}$$

and our assumption (4) yields a general polytropic equation of state of form

$$p = K\tau^{-\gamma} e^{S/c_\tau}, \tag{19}$$

with

$$\gamma = \frac{R}{c_\tau} + 1. \tag{20}$$

Here R and c_τ are defined via the ideal gas relations,

$$p\tau = RT, \tag{21}$$

$$e = c_\tau T, \tag{22}$$

and K is a constant determined by the choice of zero state of S [4, 15, 26]. The (Lagrangian) sound speed is then given by

$$c = \sqrt{-p_\tau} = \sqrt{K\gamma}\tau^{-\frac{\gamma+1}{2}} e^{S/2c_\tau}. \tag{23}$$

We now introduce the variables m and z in favor of S and τ, where

$$m = e^{S/2c_\tau}, \tag{24}$$

and

$$z = \int_\tau^\infty \frac{c}{m} d\tau = \frac{2\sqrt{K\gamma}}{\gamma - 1} \tau^{-\frac{\gamma-1}{2}}, \tag{25}$$

where we have used (23) and (24). It now follows that

$$\tau = K_\tau z^{-\frac{2}{\gamma-1}}, \tag{26}$$

$$p = K_p m^2 z^{\frac{2\gamma}{\gamma-1}}, \tag{27}$$

$$c = c(z, m) \equiv K_c m z^{\frac{\gamma+1}{\gamma-1}}, \tag{28}$$

where K_τ, K_p and K_c are constants given by

$$K_\tau = \left(\frac{2\sqrt{K\gamma}}{\gamma - 1}\right)^{\frac{2}{\gamma-1}}, \tag{29}$$

$$K_p = K K_\tau^{-\gamma}, \tag{30}$$

$$K_c = \sqrt{K\gamma} K_\tau^{-\frac{\gamma+1}{2}}. \tag{31}$$

Note that (24) and (25), together with the chain rule, imply that

$$\frac{d\tau}{dz} = -\frac{m}{c}, \tag{32}$$

$$\frac{\partial p}{\partial z}(z, m) = mc, \tag{33}$$

$$\frac{\partial p}{\partial m}(z, m) = \frac{2p}{m}. \tag{34}$$

For C^1 solutions, the Lagrangian equations (13)-(16) transform into the quasilinear system

$$z_t + \frac{c}{m} u_x = 0, \tag{35}$$

$$u_t + mcz_x + 2\frac{p}{m} m_x = 0, \tag{36}$$

$$m_t = 0, \tag{37}$$

where we have taken (37) in place of (16), valid for smooth solutions.

When either entropy or temperature are assumed constant, the entropy waves are frozen out, and the Lagrangian form of the Euler equations (9)-(11) reduces to the 2×2 p-system (13), (14), with $S = const.$, $p = p(\rho)$, c.f. [26]. In Section 3 below we assume $S = const.$ and show that for the resulting p-system the nonlinear waves cannot change their R/C-character under any sort of wave interaction. (This is the basis for the $1/t$ decay rate obtained in [9].)

3. Rarefactive and compressive simple waves. Recall that a simple wave in a two-dimensional spacetime region $(x, t) \in \Omega \subset \mathbb{R}^2$ is a solution whose image is locally one-dimensional: that is, the values $U(x, t)$ lie on a curve, which is necessarily the integral curve of the corresponding eigenvector of the flux matrix.

It is well known that entropy does not change across back and forward simple waves [26], so in order to study rarefactive and compressive simple waves, in this section we assume that S, and hence m, are constant. In this case, system (35)-(37) reduces to

$$z_t + \frac{c}{m} u_x = 0, \tag{38}$$

$$u_t + mcz_x = 0. \tag{39}$$

Let U denote the vector of states

$$U \equiv (z, u).$$

The Riemann invariants associated with system (38)-(39) are

$$r = u - mz, \tag{40}$$

$$s = u + mz, \tag{41}$$

which satisfy

$$r_t - cr_x = 0, \tag{42}$$
$$s_t + cs_x = 0. \tag{43}$$

Since the transformation $\tau \to z$ encapsulates the nonlinearity of the Riemann invariants, using (40), (41) we can identify the (z, u) and (r, s)-planes. In (z, u)-space the r-axis is upward with slope $-m$ and the s-axis is upward with slope m, as drawn in Figure 1.

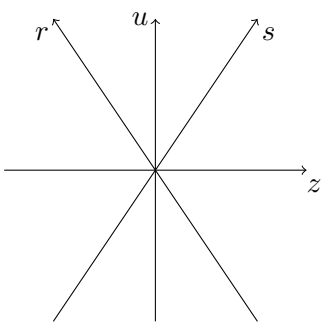

FIG. 1. *Riemann invariant coordinates.*

From (42), along backward simple waves the characteristics satisfy

$$\frac{dx}{dt} = -c, \tag{44}$$

and $r = const.$ along the characteristic, while s is constant along an opposite characteristic that passes through the wave. Thus, if subscripts L, R refer to states on the left and right of a backward simple wave, respectively, then

$$\begin{aligned} S_R &= S_L, \\ u_R - u_L &= m(z_L - z_R). \end{aligned} \tag{45}$$

Similarly, along forward simple waves the forward characteristics satisfy

$$\frac{dx}{dt} = c, \tag{46}$$

the Riemann invariant $s = const.$ along the characteristic, r is constant along an opposite characteristic that passes through the wave, and across a forward simple wave we have,

$$\begin{aligned} S_R &= S_L, \\ u_R - u_L &= m(z_R - z_L). \end{aligned} \tag{47}$$

Letting A and B denote the states ahead of and behind the wave, respectively, (so $A = L$ for a backward wave, $A = R$ for a forward wave), both (45) and (47) reduce to the *single* condition

$$\begin{aligned} S_R &= S_L, \\ u_R - u_L &= m(z_A - z_B), \end{aligned} \tag{48}$$

valid for all simple waves.

A simple wave is rarefactive (R) or compressive (C) according to whether the sound speed c decreases or increases from ahead (A) to behind (B) the wave, respectively. Since $dc/dz > 0$, it follows that in all cases a simple wave is rarefactive or compressive according to

$$\begin{aligned} \text{Rarefactive} \quad &\text{iff} \quad z_A \geq z_B, \\ \text{Compressive} \quad &\text{iff} \quad z_B \geq z_A. \end{aligned} \tag{49}$$

Note that we allow $z_A = z_B$ in both Compressive and Rarefactive waves, so that constant states can be treated as both rarefactive and compressive. The following proposition now states that the R/C character of a simple wave cannot be altered by interaction of waves at a constant entropy level:

PROPOSITION 1. *When simple waves interact at a constant entropy level, the R/C character of back/forward nonlinear waves is preserved across the interaction.*

To see this, note that it follows from (38), (39) that when waves interact, characteristics bend but states change linearly in the (z, u)-plane, or equivalently in the (r, s)-plane of Riemann invariants. This is made precise in the following North/South/East/West (NSEW) lemma, c.f. [38, 36].

LEMMA 2. *Consider two simple waves, separated by constant states at time $t = 0$, that begin interacting at time $t = t_1 > 0$, interact for time $t_1 < t < t_2$, and then separate from the interaction at time $t = t_2$. Let U_W and U_E denote the left most and right most constant states, and let U_S and U_N denote the intermediate constant states before and after interaction. Then the following relations hold:*

$$u_E - u_N = m(z_E - z_N), \tag{50}$$

$$u_N - u_W = m(z_W - z_N), \tag{51}$$

$$u_E - u_S = m(z_S - z_E), \tag{52}$$

$$u_S - u_W = m(z_S - z_W). \tag{53}$$

Proof. The interaction is depicted in Figure 3, but without the entropy jump. The lemma follows directly from our expression (48) for all simple waves. □

By eliminating u from (50)-(53), we see that the change in z across the backward and forward waves is the same before and after interaction, (e.g. $z_E - z_N = z_S - z_W$, etc.). In particular, Lemma 2 implies that the z-strength and the R/C character of simple waves is not changed across an interaction, and the Proposition follows at once.

More generally, the local R/C character of a general smooth solution can be determined from the partial derivatives r_t and s_t, as follows. Since r is constant along backward characteristics, r_t gives the change in r across the backward wave as time increases (measured along the opposite characteristic on which $s = const.$). Since

$$\frac{\partial c}{\partial z} > 0 \quad \text{and} \quad z = \frac{s - r}{2m}, \tag{54}$$

the sign of r_t determines whether c increases or decreases across the backward wave, and thus determines whether the backward wave is compressive or rarefactive. If $r_t \geq 0$, then c decreases from ahead to behind across the backward wave, so the wave is rarefactive, and if $r_t \leq 0$ the backward wave is compressive. Similarly, if $s_t \geq 0$,

the forward wave is compressive, while if $s_t \leq 0$, it is rarefactive. This then motivates the following definition:

DEFINITION 3. *The local R/C character of a general smooth interacting solution is defined (pointwise) by:*

$$\text{Forward } R \text{ iff } s_t \leq 0, \tag{55}$$
$$\text{Forward } C \text{ iff } s_t \geq 0, \tag{56}$$
$$\text{Backward } R \text{ iff } r_t \geq 0, \tag{57}$$
$$\text{Backward } C \text{ iff } r_t \leq 0. \tag{58}$$

Again, the definition allows both R and C to apply to constant states. Figure 2 depicts these regions in the $(\dot{z}, \dot{u})$ tangent plane. The following theorem makes precise the statement that rarefaction and compression is preserved for smooth solutions when the entropy is constant.

THEOREM 4. *For smooth solutions of the compressible Euler equations at a constant entropy level, the local R/C character does not change along back and forward characteristics.*

Proof. Consider a characteristic in a smooth solution at a constant entropy level. Assume without loss of generality that it is a forward characteristic. Draw a characteristic diamond in an ϵ-neighborhood of the given characteristic, and apply NSEW Lemma to see that the mapping of values of s along the transverse back characteristic at the start of the original characteristic, to values of s along the back characteristic at the end, is $1-1$ and *onto* in some ϵ neighborhood. Thus the monotonicity of s along the back characteristic transverse to the original characteristic is preserved along the original characteristic. Since characteristics always have non-zero speed, it follows directly that this monotonicity is preserved in the t direction as well, thereby proving the theorem. □

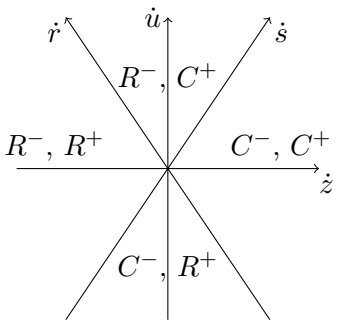

FIG. 2. *R/C character as determined by derivatives of the Riemann coordinates.*

4. The R/C structure of wave interactions at an entropy discontinuity. We now use (55)-(58) together with the Rankine-Hugoniot jump conditions to determine necessary and sufficient conditions for a nonlinear wave to change its R/C value at an entropy jump. So consider the interaction of smooth simple waves at a zero speed discontinuity in the entropy that separates constant entropy states S_L and S_R.

The Rankine-Hugoniot jump conditions[5] for discontinuous solutions of (13)-(15) are

$$\begin{aligned} \sigma[v] &= -[u], \\ \sigma[u] &= [p], \\ \sigma[E] &= [up], \end{aligned} \tag{59}$$

where σ is the speed of the discontinuity, and as usual, square brackets around a quantity denote the jump, $[f] = f_R - f_L$. For zero speed entropy waves $\sigma = 0$, (59) is equivalent to $[u] = 0 = [p]$. Thus, using (27) we rewrite the entropy jump as

$$u_L = u_R, \tag{60}$$

$$z_R = z_L \left(\frac{m_L}{m_R}\right)^{\frac{\gamma-1}{\gamma}}, \tag{61}$$

and so, by (28), also

$$m_R z_R = m_L z_L \left(\frac{m_L}{m_R}\right)^{\frac{-1}{\gamma}}, \tag{62}$$

$$c_R = c_L \left(\frac{m_L}{m_R}\right)^{\frac{1}{\gamma}}. \tag{63}$$

Now consider the interaction of two smooth simple waves at an entropy discontinuity separated by constant entropy values S_L and S_R. Assume that the nonlinear waves are separated before time $t_1 > 0$ and after time $t_2 > t_1$. Let U_W and U_E denote the left (West) most and right (East) most constant states, and let U_{SL}, U_{SR} and U_{NL}, U_{NR} denote the intermediate states between the waves on the left and right side of the discontinuity, at times $t \le t_1$ (South) and $t \ge t_2$ (North); that is, before and after interaction, respectively, as depicted in Figure 3. Now let $U_L(t)$ and $U_R(t)$ denote the values of $U = (z, u)$ on the left and right sides of the entropy jump, respectively. Then the interaction occurs for $t_1 \le t \le t_2$, and at the discontinuity we have $U_L(t_1) = U_{SL}$, $U_L(t_2) = U_{NL}$ and $U_R(t_1) = U_{SR}$, $U_R(t_2) = U_{NR}$.

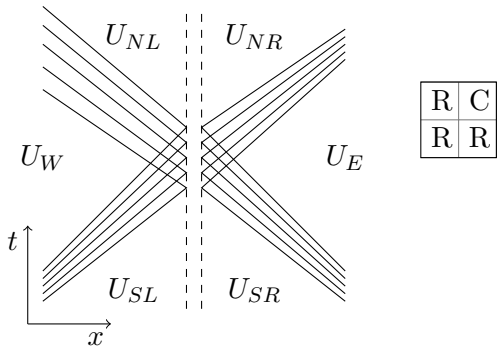

FIG. 3. *Two waves crossing at an entropy jump: when the forward wave changes from R to C, the backward wave cannot.*

[5]For weak solutions the Rankine-Hugoniot jump conditions for (13)-(15) are equivalent to the Rankine-Hugoniot jump conditions for the original Euler equations, c.f. [26, 32]

By (55)-(58), the backward wave will change its R/C value at the entropy jump iff the sign of $\dot{r} = \dot{u} - m\dot{z}$ changes across the jump, and the forward wave will change R/C character at the entropy jump iff the sign of $\dot{s} = \dot{u} + m\dot{z}$ changes sign across the jump. But by (60), (62), we have

$$u_R(t) = u_L(t), \tag{64}$$

$$m_R z_R(t) = m_L z_L(t) q_L^R, \tag{65}$$

where

$$q_L^R = \left(\frac{m_R}{m_L}\right)^{\frac{1}{\gamma}}. \tag{66}$$

Thus, for example, a backward wave changes from C to R across the entropy jump iff $\dot{r}_L = \dot{u}_L - m_L\dot{z}_L < 0$ and $\dot{r}_R = \dot{u}_R - m_R\dot{z}_R > 0$, which in light of (64), (65) is equivalent to $q_L^R m_L \dot{z}_L < \dot{u}_L < m_L\dot{z}_L$. That is, we can determine the R/C changes across the entropy jump from inequalities on the time derivative of the solution at the left hand side of the entropy jump alone. Doing this in all cases yields the following theorem. For notation let, for example, $R_{in}^+ \to C_{out}^+$ mean that the + (forward) wave changes from rarefactive (R) to compressive (C) in forward time across the entropy jump; and for example, $C_{in}^- \to R_{out}^-$, means that the − (backward) wave changes from compressive to rarefactive in forward time across the entropy jump, c.f. Figure 3. We then have the following theorem:

THEOREM 5. *A nonlinear wave changes its R/C value at an entropy jump when one of the following inequalities hold:*

$$R_{in}^- \to C_{out}^- \text{ iff} \quad q_L^R m_L \dot{z}_L < \dot{u}_L < m_L \dot{z}_L, \tag{67}$$

$$C_{in}^- \to R_{out}^- \text{ iff} \quad m_L \dot{z}_L < \dot{u}_L < q_L^R m_L \dot{z}_L, \tag{68}$$

$$R_{in}^+ \to C_{out}^+ \text{ iff} \quad -q_L^R m_L \dot{z}_L < \dot{u}_L < -m_L \dot{z}_L, \tag{69}$$

$$C_{in}^+ \to R_{out}^+ \text{ iff} \quad -m_L \dot{z}_L < \dot{u}_L < -q_L^R m_L \dot{z}_L. \tag{70}$$

Now note that dividing the inequalities in (67)-(70) through by $\dot{z}$, we obtain bounds on the derivative $\frac{du}{dz} = \frac{\dot{u}_L}{\dot{z}_L}$ on the left hand side of the entropy jump that determine exactly when a wave changes its R/C character. Of course, the inequalities change depending on whether $\dot{z} < 0$ or $\dot{z} > 0$.

More generally, consider the lines through the origin of slope $\pm m_L$ and $\pm q_L^R m_L$ in the $(\dot{z_L}, \dot{u_L})$-plane. These determine the boundaries between eight angular wedges, in each of which the R/C character of the interactions is constant. That is, the R/C character of incoming and outgoing waves on both sides of the jump are determined in each of these wedges. There are two cases, depending on whether q_L^R given by (66) is smaller or larger than unity, which is just whether $m_L < m_R$ or $m_L > m_R$. In other words, the eight angular regions in the $(\dot{z}, \dot{u})$-plane, determine the signs of the derivatives of the Riemann invariants $\dot{r}$ and $\dot{s}$ uniquely on both sides of the entropy jump. The signs of $\dot{r}$ and $\dot{s}$ in each region are determined by inequalities similar to (67)-(70) that follow from the relations between (u, z) and (r, s) together with the jump relations (64), (65). These regions, together with the R/C character of the interactions in each region, are diagrammed for the cases $m_L < m_R$ and $m_R < m_L$ in Figures 4 and 5, respectively.

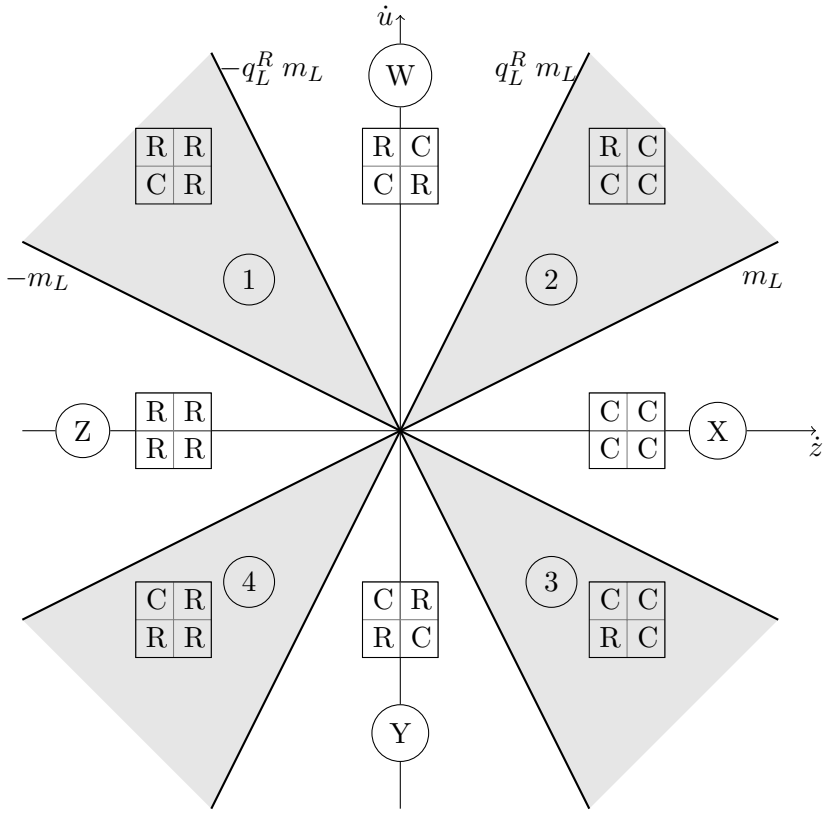

FIG. 4. *Tangent space showing the possible R/C wave structures when $m_L < m_R$.*

Each separate region in Figures 4 and 5 is labeled by a box containing four values among R and C that label the R/C value of the wave in the corresponding position in Figure 3. For example, the upper right hand value of R/C corresponds to the outgoing forward wave, and the lower right hand value in each box corresponds to the incoming backward wave, etc. We will refer to the interaction types in Figures 4 and 5 by the circled numbers and letters that appear in each region of the diagrams. Interactions in which there is an R/C change along one of the diagonals are labeled with numbers (numbers $1-4$ appear in Figure 4, clockwise; numbers $5-8$ appear in Figure 5, counterclockwise), while the interactions in which there is no R/C change along a diagonal are labeled with letters W, X, Y, Z.

Note that only twelve of the sixteen possible assignments of R/C to the four entries of the box actually appear in some region. The ones that do not appear are exactly the cases in which both the forward and backward waves change their R/C values simultaneously at the interaction. From this we conclude that this type of interaction is not possible; i.e., a wave can change its R/C value only if a wave from the opposite nonlinear family transmits its R/C value through the interaction at the same time. This reflects the fact that the inequalities (67)-(70) are mutually exclusive: that is, at most one of them can hold.

5. The simplest periodic structure. Using Figures 4 and 5, and after some work, we find the simplest periodic array of R's and C's consistent with the condition

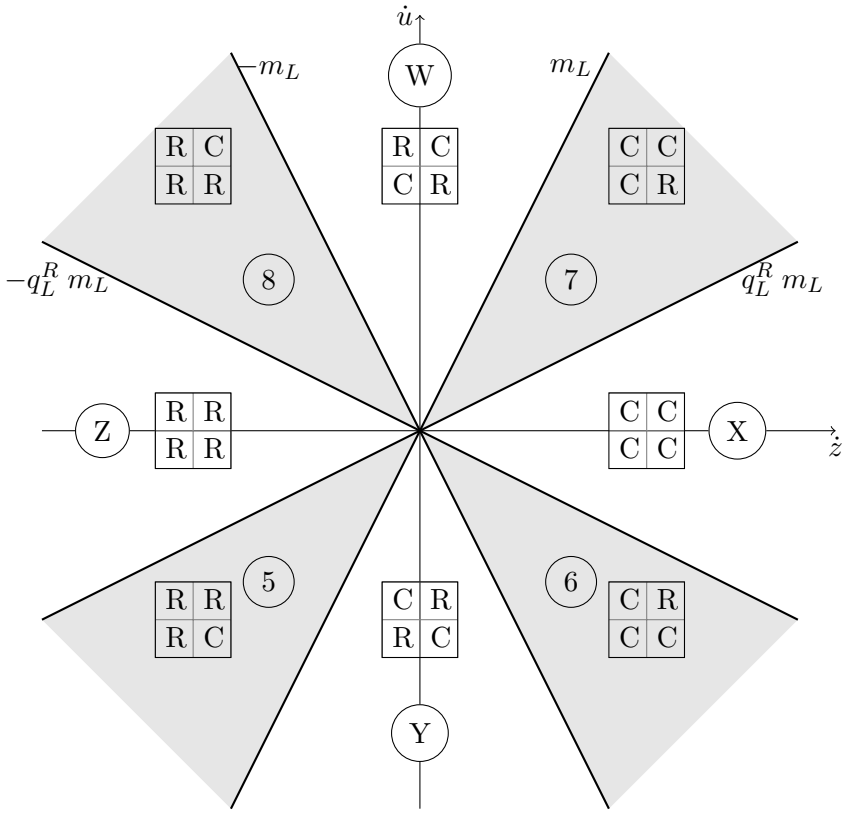

FIG. 5. *Tangent space showing the possible R/C wave structures when* $m_L > m_R$.

that there is an equal number of R's and C's along every (characteristic) diagonal, and such that at the center of every box of R's and C's we obtain a consistent label for a box associated with some interaction diagrammed in Figure 4 or 5. This simplest formal pattern is diagrammed in Figure 6, and is based on two alternating entropy levels. To interpret Figure 6, note that the darker vertical lines represent the entropy jumps in the (x, t)-plane, and at this stage the backward and forward "characteristics" are formally represented as moving at constant speed ± 1 through the centers of the circles.

Two alternations of entropy, yielding four separate entropy levels, are depicted in Figure 6. The number in the circle at the center of each R/C box in Figure 6, agrees with the number that labels the corresponding interaction in Figure 4 or 5. Consistent with our results of Section 4, the boxes of Figure 4 or 5 in which R or C change along a diagonal, labeled with *numbers*, appear only at the entropy jumps. For the wave interaction boxes at constant entropy, away from the entropy jumps, (labeled by *letters*), both R and C are transmitted along back/forward characteristics through the diagonals of the box. Figure 6 depicts one tile of a periodic configuration, and this tile repeats with a one-half period shift in space for every time period. To generate the tiling, slide the bottom left corner of the tile, (labeled by the shaded circled number 1), up and to the right until it is aligned with the corresponding shaded circled number 1 in the middle of the top of the tile. It is not difficult to see that this motion generates a periodic structure. The "characteristics" in Figure 6, regarded as the diagonal lines

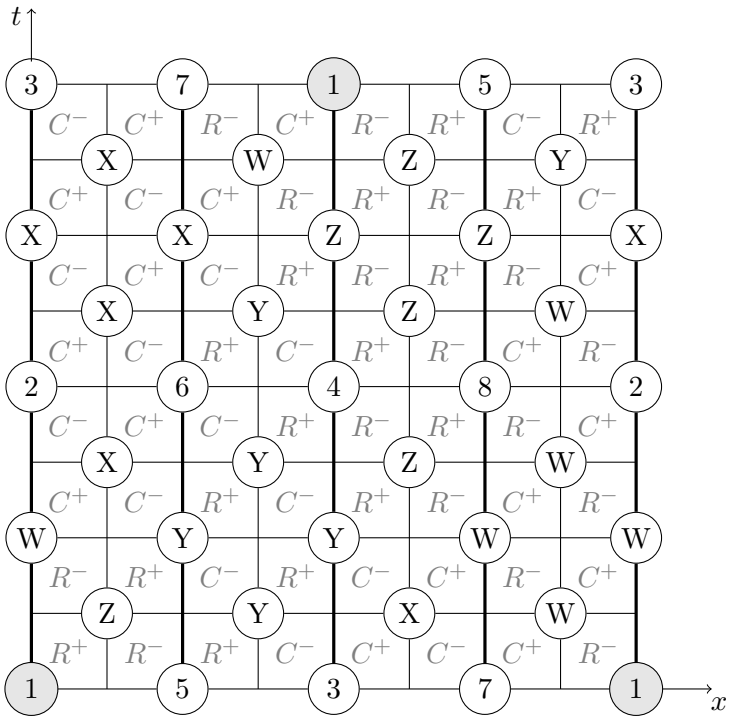

FIG. 6. *The simplest R/C pattern consistent with Figures 4 and 5, in which R and C are in balance along every + and − characteristic.*

that pass through the centers of circled labels, are labeled with R's and C's according to whether a real characteristic would be rarefactive or compressive at the circled interaction, and the superscript $\pm$ is appended to identify back/forward directions, respectively. Note that each $\pm$ "characteristic" diagonal traces four R's and four C's, each at a constant entropy level, before returning to its starting value. (By this count we identify R's and C's on opposite sides of lettered interactions at constant entropy.) Note that the half period shift contributes to mixing of R's and C's along characteristic diagonals.

We now argue that the R/C pattern in Figure 6 is consistent with a global periodic structure of states and characteristics in the (x,t)-plane, such that the actual compression and rarefaction of the characteristics in the (x,t)-plane is consistent with the R/C pattern of Figure 6. One can see how to accomplish this once one notices that the ordering of the wave interaction types in time along the left and right sides of each entropy jump in Figure 6, is consistent with derivatives going around an (approximately) elliptical shaped curve that cycles once around every time period. The direction of rotation in (z,u)-space is reversed on opposite sides of each entropy level, but the rotation direction is the same on the left and right sides of each entropy jump. Such elliptical shaped curves would have maximum and minimum values of r and s once in each period, and in an actual solution, these would mark the boundaries between the rarefactive and compressive regions of the solution. Putting this together, we are led to the "cartoon" of a time periodic solution depicted in Figures 7 and 8. The depiction of several tiles set within the global periodic structure is given in Figure 9.

Figure 7 gives a detailed picture of a proposed periodic solution that produces the

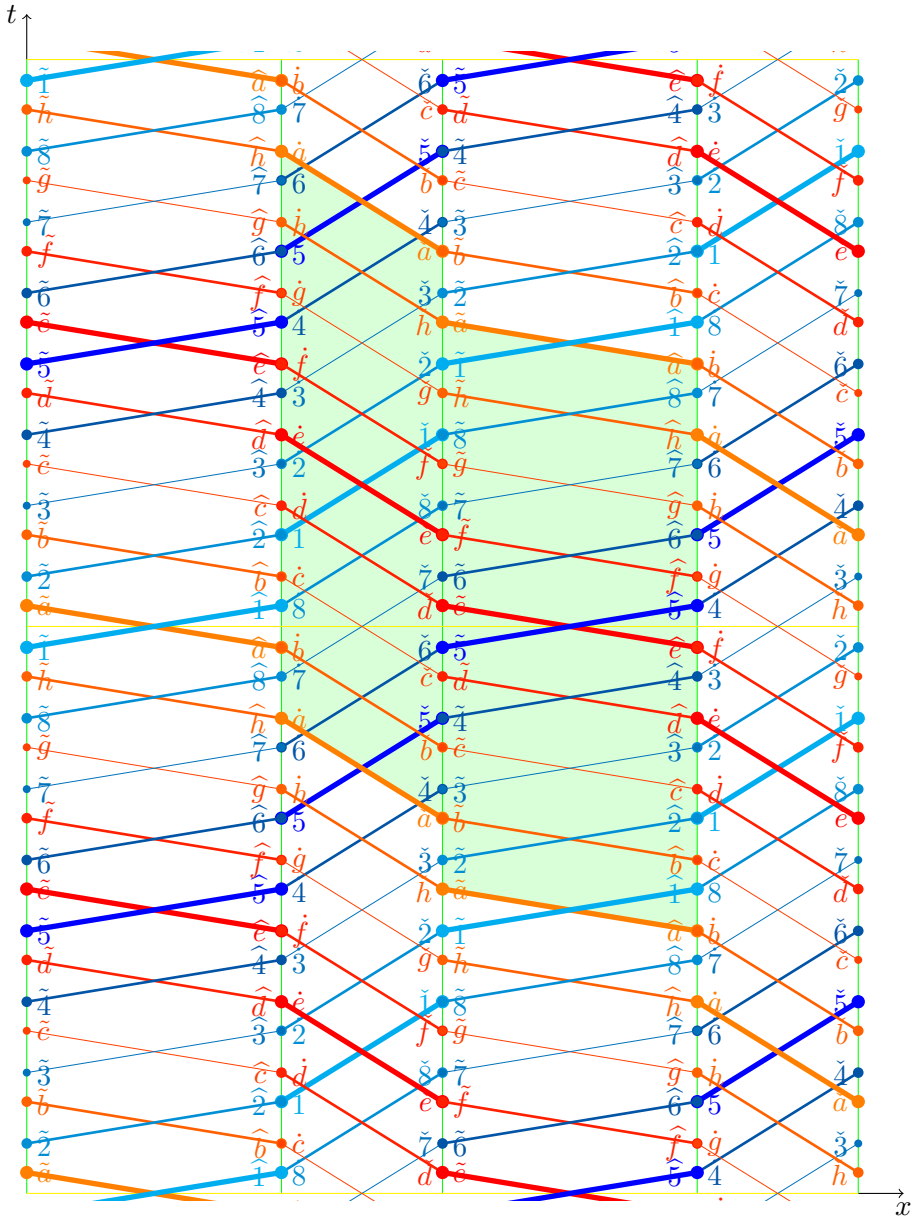

FIG. 7. *The characteristic structure of our time-periodic solutions in the* (x,t)*-plane.*

R/C pattern of Figure 6. The letters and numbers in Figure 7 give the (x,t) positions of the approximate corresponding states labeled in Figure 8, these states becoming exact as the solution at each entropy level tends to a constant state. Figure 9 depicts the periodic tiling of the (x,t)-plane obtained by extending Figure 7 periodically[6].

[6]In fact, we originally constructed Figures 7-8 from the pattern of Figure 6 alone. However, in our forthcoming paper [29], we derive exact formulas for solutions of the linearized problem that generates Figures 7 and 8 *exactly*, and show that the nonlinear problem can be recast as a perturbation from these.

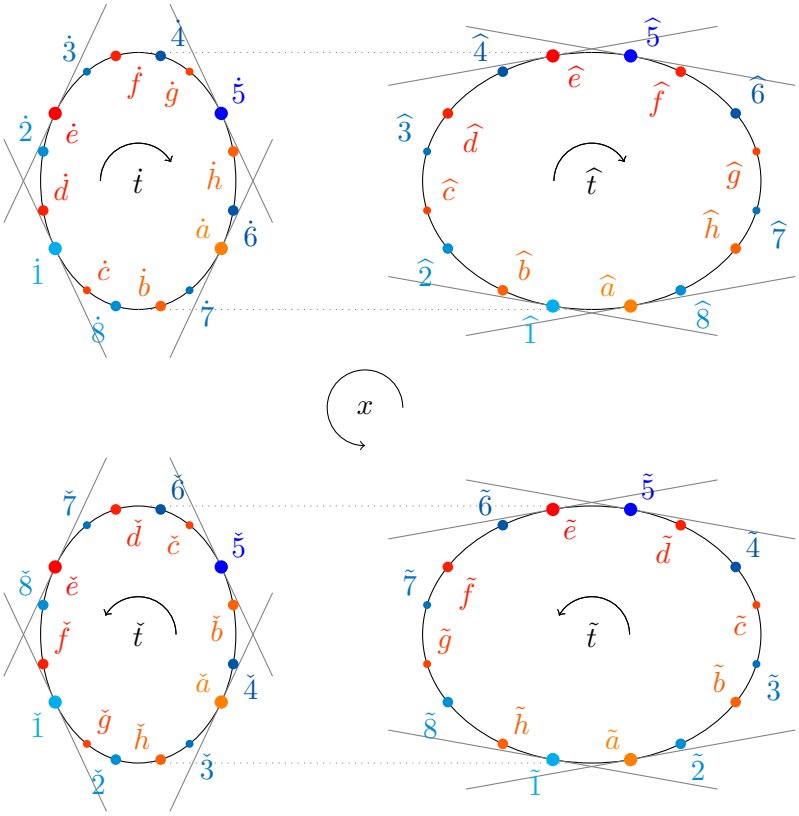

FIG. 8. *Ellipses showing periodicity in the* (z, u)*-plane.*

Figures 7-9 strongly indicate the consistency of the periodic pattern displayed, but of course the actual existence of a periodic solution like this that solves the Euler equations exactly, remains to be proven.

In Figure 7, the vertical lines mark the entropy jumps, and the solutions on the left and right of one entropy jump are labeled $\check{U} \mid \dot{U}$, and labeled $\check{U} \mid \tilde{U}$ on the other, respectively. The solution alternates between two different entropy values $\underline{m} < \overline{m}$. The wider entropy level depicted in Figure 7 corresponds to the smaller value $\underline{m}$, where, consistent with (63), we have depicted characteristics with faster speeds. The diagonal lines rising to the left and right through the entropy levels mark the back and forward characteristics, respectively. The thicker characteristics mark the maximum and minimum values of r and s at each entropy level, these values propagating along back and forward characteristics, respectively. We call these the *max/min* characteristics. In an actual solution, the back characteristics would be rarefying where $r_t > 0$ and compressing where $r_t < 0$, while the forward characteristics would be compressing where $s_t < 0$ and rarefying where $s_t > 0$, but our cartoon in Figure 7 depicts a linearized version of a solution in which characteristics are drawn with the constant speed on each entropy level, c.f. (55)-(58). Note that it is the disconnections between *max/min* characteristics at the entropy jumps that produces the regions where characteristics change from R to C, or vice versa. The solution is consistent with elliptical shaped curves in (z, u)-space defining values of the solution

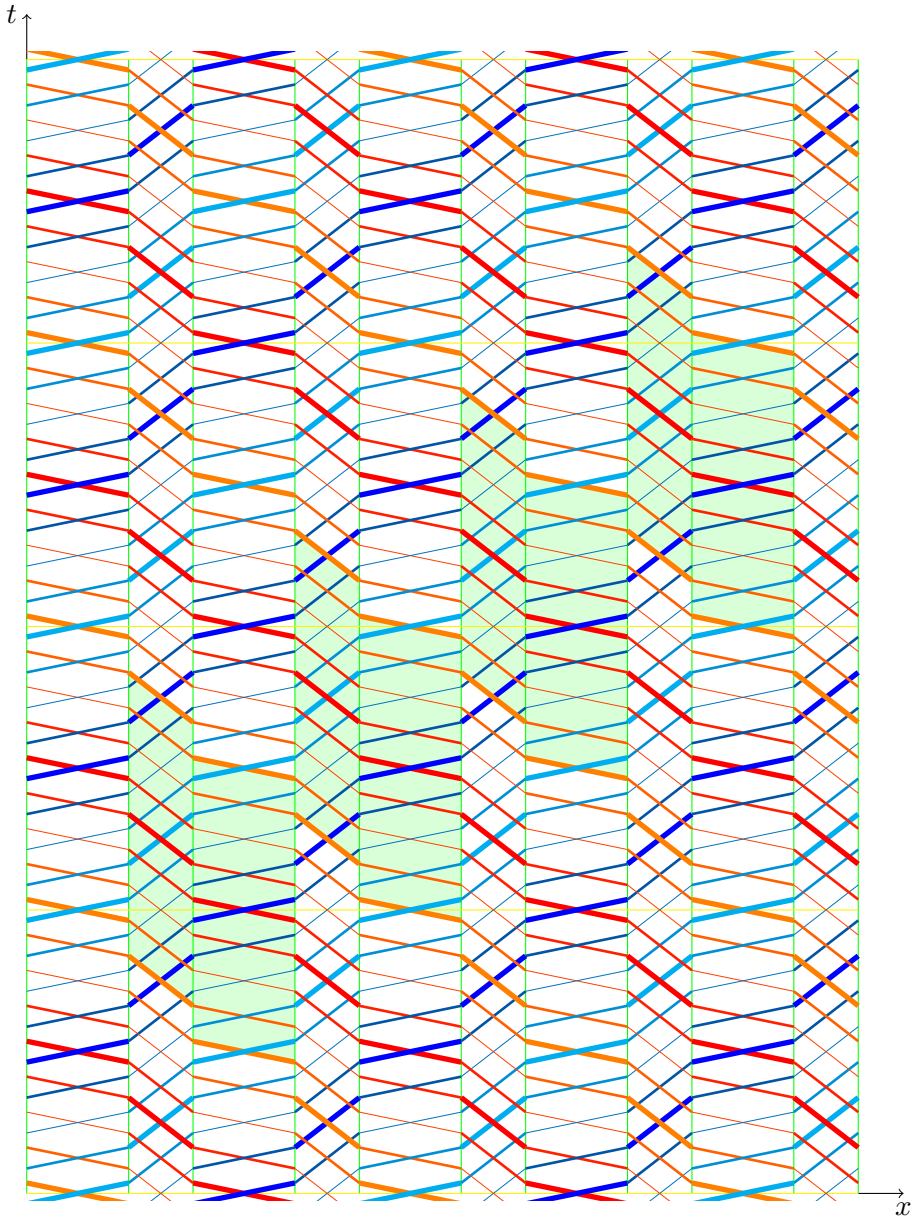

FIG. 9. *A single tile set within the global periodic structure of the* (x,t)*-plane.*

on each side of the entropy jumps, depicted in Figure 8. The tangents of slope $\pm\underline{m}$ and $\pm\overline{m}$ in Figure 8 label the *max/min* values of $r = const.$ and $s = const.$ at each entropy level. Note that Figure 8 shows the (z,u)-plane, while Figures 4 and 5 show the (tangent) $(\dot{z},\dot{u})$-plane. Thus, e.g., the arc $\check{1}$–$\check{2}$ in the bottom left ellipse corresponds to region 6 in Figure 5, with $m_L = \overline{m} > \underline{m} = m_R$. Again, we show in [29] that Figure 8 is exact for the linearized problem in which wave speeds are assumed constant on each entropy level, which is the limit of small perturbations of a piecewise constant solution.

The letters and numbers in Figure 8 label the (z,u)-state values at the corresponding locations along the vertical entropy jumps labeled in Figure 7. Note that the numbers increase consecutively in forward time along the forward characteristics in Figure 7, and the letters increase consecutively in forward time along the backward characteristics. The minimum, maximum value of r occurs along the backward min, max characteristic labeled by letters a and e, respectively; and the minimum, maximum value of s occurs along the forward min, max characteristic labeled by numbers 1 and 5, respectively. Letters and numbers are adorned with $\check{}\,|\,\tilde{}$ and $\hat{}\,|\,\dot{}$ at the left and right sides of the $\overline{m}\mid\underline{m}$ and $\underline{m}\mid\overline{m}$ entropy jumps, respectively. The max/min letters and numbers determine state values across the entropy jumps via the jump conditions (64), (65). The remaining lettered and numbered states in Figures 7, 8 are determined by characteristic connections across entropy levels, (r and s are constant along backward and forward characteristics, respectively), and the jump relations across the entropy jumps. That all states lie exactly on the elliptical curves of Figure 8 assumes that Figure 7 really is a consistent solution. As we have noted, we show in [29] that Figure 8 is correct in the limit of constant wave speeds at each entropy level, but in an actual solution the states in Figure 8 would lie on curves that are perturbations of true ellipses. Note that we imposed the labeling condition that letters and numbers would increase by one at entropy jumps along characteristics moving forward in time. Thus one can trace the evolution of the states along a characteristic by following the consecutive numbers/letters around the elliptical curves of Figure 9. One can also verify that the corresponding labels moving vertically along one side of an entropy jump traverse the elliptical curves of Figure 8 in clockwise or counterclockwise order. This is then a *consequence* of the pattern, and strongly indicates the consistency of the pattern with an actual solution. Moreover, the fact that the elliptical curves are traversed in opposite directions in the (z,u)-plane on opposite sides of the same entropy level is consistent with the assumption that back and forward max/min characteristics cross exactly once in each level, so the evolution creates an inversion of the curve at each level. In [29] we will see that this corresponds to a quarter period evolution of an exact periodic elliptical solution of the linearized problem.

Note that in Figure 7 the speed of the wave crests is determined by the speed of the max/min characteristics, which is interpreted as the speed of the period. This is slower than the speed of the characteristics (the sound speed), due to the fact that corresponding characteristics are disconnected at each entropy jump, and always jump *up* in *forward* time. Thus the speed of the period, which is the effective speed of these waves, is *subsonic*. We have thus identified *two* distinct wavespeeds in our solution: the speed of the period, which is like a group velocity, and the characteristic speed, which is like a phase velocity. To our knowledge, this is the first time such a phenomenon has been identified in a purely quasilinear hyperbolic system. The corresponding supersonic waves having the structure of our solutions appear to be ruled out by the asymmetries in Figures 3,4 with respect to $m_R < m_L$ and $m_R > m_L$.

Note also that in Figure 7 we have depicted the traces of the max/min characteristics joining every four entropy levels. This is a simplifying assumption that need not hold in a general periodic solution having the R/C structure of Figure 6. The effect of this merging of max/min characteristics every four entropy levels is to partition the solution into four regions of rarefaction and four regions of compression in each period of each entropy level. By propagating these regions forward in time along characteristics, we see that each such region cycles upward through four consecutive

regions of rarefaction and four consecutive regions of compression before returning to its original position in the tile. This makes for a clear image of how the solution in Figure 7 is propagating.

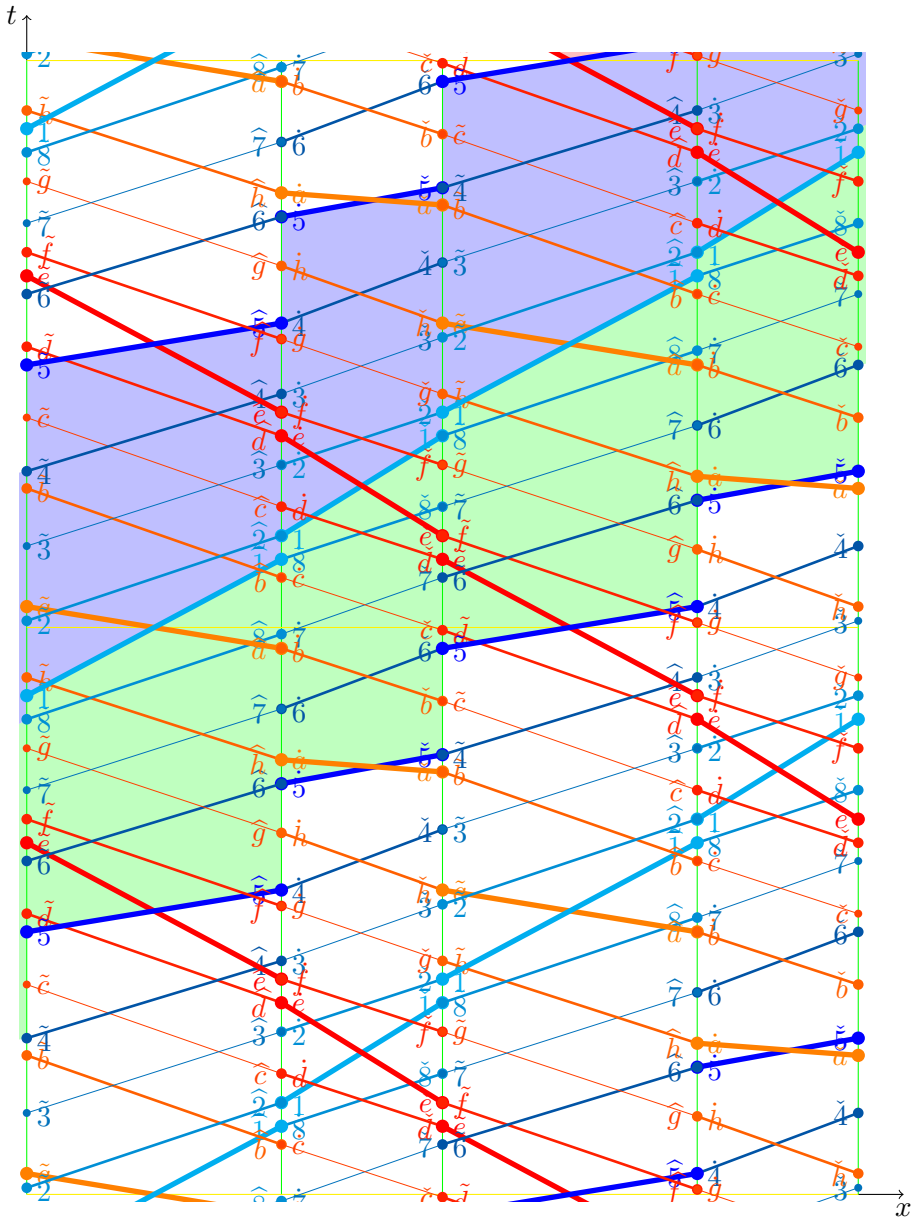

FIG. 10. *A periodic pattern incorporating compression and rarefaction.*

The "solution" diagrammed in Figures 7, 8 is a cartoon only because the wave speeds are not propagating at the exact speed of an exact state assigned to the solution, and the actual values in the solution will depend on the time periodic elliptical shaped curve along an entropy level that can serve as an initial condition for the subsequent evolution in space by (35)-(37). In Figure 7, the characteristic speeds

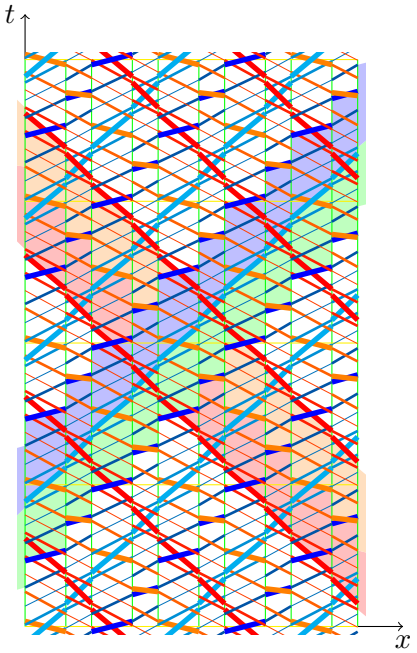

FIG. 11. *The global nonlinear periodic structure in the* (x,t)*-plane.*

are drawn as constant in each entropy level. We show in [29] that this is exact for the linearized problem. But in a nonlinear problem, the back characteristic speeds would be compressive/rarefactive between the max/min and min/max back characteristics, respectively, and forward characteristics would be compressive/rarefactive between max/min and min/max characteristics, respectively. To further demonstrate the consistency of this periodic pattern, in Figures 10 and 11 we have drawn a periodic pattern respecting the overall structure of Figures 7 and 8, but such that it correctly reflects the compression and rarefaction of characteristics in each entropy level.

Figures 10 and 11 are only cartoons because wave speeds are not propagating at the exact speed of the state assigned to the solution. However, the fact that such a cartoon can be drawn as exactly periodic for a consistent choice of wave speeds that correctly reflect compression and rarefaction, the fact that rarefaction and compression is balanced along every characteristic in the diagram[7] and the fact that there are so many degrees of freedom in the drawing that can be changed while preserving this periodic structure, convinces us that true time periodic solutions of (35)-(37) exhibiting this structure, actually exist. A complete mathematical proof of this is the subject of the authors' ongoing research.

6. Conclusion. It is the conjecture of the authors that a large class of solutions of the compressible Euler equations starting from space periodic initial data, will ultimately decay in time to a solution that balances compression and rarefaction along characteristics, like the solutions constructed here. We conceive of the mechanism that drives this as follows: if the initial data is not perfectly tuned to a given initial entropy profile, then in general shock-waves will form, thereby introducing new entropy states.

[7] Also, these diagrams represent small perturbations of a linearized solution that exhibits the structure exactly [29].

The entropy field will then evolve in time as the shock-waves interact and dissipate entropy, and the solution will decay until it finds a balance between compression and rarefaction along characteristics, analogous to what we found here. We expect that there is a rich, and yet to be found, mathematical structure that describes, in patterns of R's and C's, all of the ways that a nonlinear periodic solution can balance compression and rarefaction along characteristics, the solutions presented here being the simplest. If correct, this raises a host of fascinating questions, the first one being how to give a mathematically complete proof that solutions with this global nonlinear structure do indeed solve the Euler equations exactly.

In [29] we describe and solve the linearized problem associated to nonlinear periodic solutions having the structure described in this paper. We prove that the periodic solutions with this structure are isolated in a one-mode kernel of the linearized operator, and completely characterize the spectrum. In particular, we show that the linearized operator is bounded, invertible and diagonal on the complement of its kernel, with inverse bounded on all but a sparse set of modes associated to small divisors. In [30], we show that a Liapunov-Schmidt decomposition reduces the problem to an Implicit Function Theorem for an invertible (non self-adjoint) operator having small divisors. In addition, we prove that periodic solutions with the wave structure derived here exist to within arbitrarily high Fourier mode cutoff. Taken all together, we believe this constitutes what we might call a "physical" proof that periodic solutions having the wave structure we have identified exist. The main technical obstacle to a complete proof is the existence of resonances and small divisors for periodic solutions in a *quasi-linear hyperbolic* problem[8], which to our understanding, is beyond the present limits of mathematical technology, c.f. [7, 1], and [23, 5, 2, 39] for applications to *semi-linear* problems. However, in our view, the history of KAM theory indicates that one can only expect that these technical difficulties can be overcome.

If these periodic structures are realized in exact solutions of the compressible Euler equations, one can ask, is there a sense in which they are stable? Will nearby space periodic data decay to nearby time periodic solutions? Are there periodic solutions that are stable within the class of *smooth* solutions? Do there exist quasi-periodic solutions, and would these be attractors for other solutions with more general data? We believe the phenomenon of balancing compression and rarefaction is stable even if individual solutions are not. If solutions are unstable, could this herald the onset of chaotic or turbulent behavior? Perturbation of unstable rest points leads to bifurcation, period doubling, and the onset of chaos in dynamical systems, so could these simplest periodic wave structures be a doorway to the study of similar complicated phenomena in the compressible Euler equations? Are there counterexamples? Is the theory of approximate characteristics developed to prove decay to shock-waves, N-waves and solutions of the Riemann problem in compactly supported solutions, sufficient to prove decay to periodic solutions? Is there a Glimm type potential interaction term that measures the degree to which compression and rarefaction is *not* balanced at a given time, (something like the potential in the method of re-orderings, [33, 28]), that could estimate the evolution of a small perturbation from periodic data [8, 6, 18, 26]? Estimating how such a potential evolves might control the potential for future shock-wave production. One advantage here is that the total entropy is non-increasing, so there is *a priori* control over the evolving entropy profile.

It is our view that the work here provides a paradigm for how, when entropy

[8]These arise in the spectrum of the linearized operator for reasons analogous to the inability to bound irrational maps of the circle away from rational numbers, [29].

variations are present, nonlinear sound waves can get into configurations of balancing compression and rarefaction, and thereby prevent the $1/t$ attenuation rate of shock-wave dissipation from taking hold. This implies that signals can propagate much further than the theory has suggested so far, and this applies not only to weak waves, but to strong waves too. According to folklore in the subject of conservation laws, the then unexplained attenuation in sonar signals during World War II was later explained by the $1/t$ decay rate due to shock-wave dissipation proved in [9]. This analysis neglected entropy variations. Could it be that when temperature and entropy variations are present, sound waves can travel much further without dissipation by finding a configuration that balances compression and rarefaction like the waves we construct here? For example, in turbulent air, sound seems to carry further, and it is well known that whales can communicate over very long distances. Could this kind of long distance signaling be taking advantage of the phenomenon described here? In principle, this is a testable hypothesis, as, for example, there is a difference in speed between the periodic shock-free waves constructed here and the classical sound and shock speeds.

REFERENCES

[1] S. Alinhac and P. Gerard, *Pseudo-differential operators and the Nash-Moser theorem*, Graduate Studies in Math., no. 82, Amer. Math. Soc., Providence, 2007.

[2] J. Bourgain and W. Wang, *Quasi-periodic solutions of nonlinear lattice Schrodinger equations with random potential*, J. Euro. Math. Soc., 10 (2008), pp. 1–45.

[3] D. Christodoulou, *The Euler equations of compressible fluid flow*, Bull. Amer. Math. Soc., 44 (2007), pp. 581–602.

[4] R. Courant and K. O. Friedrichs, *Supersonic flow and shock waves*, Wiley, New York, 1948.

[5] W. Craig and G. Wayne, *Newton's method and periodic solutions of nonlinear wave equations*, Comm. Pure Appl. Math., 66 (1993), pp. 1409–1498.

[6] C. M. Dafermos, *Generalized characteristics in hyperbolic systems of conservation laws*, Arch. Rat. Mech. Anal., 107 (1989), pp. 127–155.

[7] K. Deimling, *Nonlinear functional analysis*, Springer, 1985.

[8] J. Glimm, *Solutions in the large for nonlinear hyperbolic systems of equations*, Comm. Pure Appl. Math., 18 (1965), pp. 697–715.

[9] J. Glimm and P. D. Lax, *Decay of solutions of systems of nonlinear hyperbolic conservation laws*, Memoirs Amer. Math. Soc., 101 (1970).

[10] J. M. Greenberg, *Smooth and time–periodic solutions to the quasilinear wave equation*, Arch. Rat. Mech. Anal., 60 (1975), pp. 29–50.

[11] J. M. Greenberg and M. Rascle, *Time–periodic solutions to systems of conservation laws*, Arch. Rat. Mech. Anal., 115 (1991), pp. 395–407.

[12] F. John, *Formation of singularities in one-dimensional nonlinear wave propagation*, Comm. Pure Appl. Math., 27 (1974), pp. 377–405.

[13] P. D. Lax, *Development of singularities of solutions of nonlinear hyperbolic partial differential equations*, Jour. Math. Physics, 5 (1964), pp. 611–613.

[14] ———, *Hyperbolic systems of conservation laws and the mathematical theory of shock waves*, SIAM, Philadelphia, 1973.

[15] R. J. LeVeque, *Numerical methods for conservation laws*, Birkhauser, New York, 1992.

[16] T.-T. Li, Z. Yi, and K.-D. Xing, *Global classical solutions for general quasilinear hyperbolic systems with decay initial data*, Nonlinear Analysis, Theory, Methods and Applications, 28 (1997), pp. 1299–1332.

[17] T.-P. Liu, *Development of singularities in the nonlinear waves for quasi-linear hyperbolic partial differential equations*, J. Diff. Eqns, 33 (1979), pp. 92–111.

[18] ———, *Quasilinear hyperbolic systems*, Commun. Math. Phys., 68 (1979), pp. 141–172.

[19] A. Majda, *Compressible fluid flow and systems of conservation laws in several space variables*, Applied Mathematical Sciences, no. 53, Springer-Verlag, 1984.

[20] A. Majda and R. Rosales, *Resonantly interacting weakly nonlinear hyperbolic waves I. A single space variable*, Stud. Appl. Math., 71 (1984), pp. 149–179.

[21] A. Majda, R. Rosales, and M. Schonbeck, *A canonical system of integrodifferential equa-*

tions arising in resonant nonlinear acoustics, Stud. Appl. Math., 79 (1988), pp. 205–262.
[22] R. L. Pego, *Some explicit resonating waves in weakly nonlinear gas dynamics*, Studies in Appl. Math., 79 (1988), pp. 263–270.
[23] P. H. Rabinowitz, *Periodic solutions of nonlinear hyperbolic partial differential equations*, Comm. Pure Appl. Math., 20 (1967), pp. 145–205.
[24] B. Riemann, *The propagation of planar air waves of finite amplitude*, Classic Papers in Shock Compression Science (J.N. Johnson and R. Cheret, eds.), Springer, 1998.
[25] M. Shefter and R. Rosales, *Quasiperiodic solutions in weakly nonlinear gas dynamics.*, Studies in Appl. Math., 103 (1999), pp. 279–337.
[26] J. Smoller, *Shock waves and reaction-diffusion equations*, Springer-Verlag, New York, 1982.
[27] B. Temple and R. Young, *The large time existence of periodic solutions for the compressible Euler equations*, Matemática Contemporânea, 11 (1996), pp. 171–190.
[28] ———, *The large time stability of sound waves*, Comm. Math. Phys., 179 (1996), pp. 417–466.
[29] B. Temple and R. Young, *Time-periodic linearized solutions of the compressible Euler equations and a problem of small divisors*, SIAM Journal of Math Anal (2009), To appear, 54 pages, available at `http://www.math.ntnu.no/conservation/2008/034.html`.
[30] ———, *A Liapunov-Schmidt reduction for time-periodic solutions of the compressible Euler equations*, Submitted, 40 pages, available at `http://www.math.ntnu.no/conservation/2008/035.html`, 2009.
[31] D. Vaynblat, *The strongly attracting character of large amplitude nonlinear resonant acoustic waves without shocks. a numerical study*, Ph.D. thesis, M.I.T, 1996.
[32] D. Wagner, *Equivalence of the Euler and Lagrangian equations of gas dynamics for weak solutions*, Jour. Diff. Equations, 68 (1987), pp. 118–136.
[33] R. Young, *Sup-norm stability for Glimm's scheme*, Comm. Pure Appl. Math., 46 (1993), pp. 903–948.
[34] ———, *Exact solutions to degenerate conservation laws*, SIAM J. Math. Anal., 30 (1999), pp. 537–558.
[35] ———, *Periodic solutions for conservation laws*, Contemp. Math. ,255 (2000), pp. 239–256.
[36] ———, *The p-system II: The vacuum*, Evolution Equations (Warsaw) (R. Picard, M. Reissig, and W. Zajaczkowski, eds.), Banach Center, 2001, pp. 237–252.
[37] ———, *Sustained solutions for conservation laws*, Comm. PDE, 26 (2001), pp. 1–32.
[38] ———, *Global wave interactions in isentropic gas dynamics*, Submitted, 47 pages, available at `http://www.math.ntnu.no/conservation/2008/032.html`, 2008.
[39] E. Zehnder, *Generalized implicit function theorems with applications to some small divisor problems*, Comm. Pure Appl. Math., 28 (1975), pp. 91–140.